Chemical behavior and in vitro activity of mixed phosphine gold(I) compounds on melanoma cell lines.

Journal:	*Journal of Medicinal Chemistry*
Manuscript ID:	jm-2007-00978a.R2
Manuscript Type:	Article
Date Submitted by the Author:	19-Dec-2007
Complete List of Authors:	Caruso, Franco; Istituo Chimica Biomolecolare, c/o University of Rome Pettinari, Claudio; Universita di camerino, Chimica Paduano, Francesco; Istituto Tumori Villa, Raffaella; Istituto Tumori Marchetti, Fabio; Universita di Camerino Monti, Elena; Universita Insubria Rossi, Miriam; Vassar College

Chemical behavior and in vitro activity of mixed phosphine gold(I) compounds on melanoma cell lines.

Francesco Caruso,[†]* Claudio Pettinari, [§]*, Francesco Paduano,[⊥] Raffaella Villa,[⊥] Fabio Marchetti,[§] Elena Monti[#], Miriam Rossi[‡]

AUTHOR ADDRESS

[†] Istituto di Chimica Biomolecolare, Consiglio Nazionale delle Ricerche (CNR), c/o University of Rome Istituto Chimico, Piazzale Aldo Moro 5, 00185, Rome, Italy; [§] Dipartimento di Scienze Chimiche, Università di Camerino, via S. Agostino 1, 62032 Camerino, MC, Italy; [‡] Vassar College, Department of Chemistry, Poughkeepsie, NY, 12604-0484, USA; [⊥] U.O. 10, Dipartimento Sperimentale, Fondazione IRCCS "Istituto Nazionale dei Tumori", Via Venezian 1, 20133 Milan, Italy; [#] Dipartimento di Biologia Strutturale e Funzionale, Università dell'Insubria, Via A. da Giussano, 12, 21052 Busto Arsizio,VA, Italy.

AUTHOR EMAIL ADDRESS

F. Caruso: email, caruso@vassar.edu C. Pettinari: email claudio.pettinari@unicam.it

CATEGORY: Antibiotics and Chemotherapeutics

TITLE RUNNING HEAD

Mixed phosphine gold cytotoxic activity

ABBREVIATIONS. DPPP: 1,3-bis(diphenylphosphino)propane. DIPHOS: 1,2-bis(diphenylphosphino)ethane. DMPP: 1,3-bis(dimethylphosphino)propane

ABSTRACT

^{31}P-NMR and ESI-MS on the melanoma cytotoxic chlorotriphenylphosphine-1,3-bis(diphenylphosphino)propanegold(I), [Au(DPPP)(PPh_3)Cl], show partial decomposition that includes the novel dinuclear cation $[Au_2(DPPP)_2Cl]^+$; its structure was calculated using DFT. Unexpectedly, using the diphosphine ligand 1,2-bis(diphenylphosphino)ethane (DIPHOS), [{AuCl(PPh_3)}$_2$(μ_2-DIPHOS)] was obtained. Its X-ray crystal structure shows a unique triangular coordination sphere in contrast to T-shaped geometry of related gold(I)-DIPHOS compounds. Its cytotoxic activity in JR8, SK-Mel-5 and 2/60 melanoma cell lines is dose-dependent and lower than [Au(DPPP)(PPh_3)Cl] due to its non-chelating nature. An *in vitro* study of both gold compounds on the B16V melanoma cell line gives credence to this structure-activity relationship. IC_{50} indicate that both gold species are 10 times more active in B16V than in JR8, SK-Mel-5 and 2/60. Oxidation of [Au(DPPP)(PPh_3)Cl] towards Au(III) compounds and phosphine-oxides is observed upon reaction with hypochlorite in water/DMSO solution, mimicking endogenous hypochlorite. A related reaction involving the formation of $[AuCl_4]^-$ is thermodynamically feasible according to DFT calculations.

KEYWORDS

Melanoma, gold, phosphine, crystal structure, ESI-MS, DFT

INTRODUCTION

There is much interest in the research of metal complexes as potential anticancer agents. Clinical use of cisplatin has induced the ongoing investigation of alternative metal-based anticancer agents, in the hope that metal centers other than platinum might produce specific and/or improved *in vitro* and *in vivo* anticancer effects and be developed as useful drugs.[1-2] The clinically established antiarthritic gold(I) species auranofin, (1-thio-beta-D-glucopyranosato)(triethylphosphine)gold 2,3,4,6-tetraacetate), and some other gold-phosphine compounds show significant antitumor properties, both *in vitro* and *in vivo*.[3-4] Gold(I) complexes containing diphosphine ligands show greatest antitumor activity *in vitro* and *in vivo* in P388 and L1210 leukemias, M5076 reticulum cell sarcoma, B16 melanoma and Lewis lung carcinoma.[5-8]

The site where gold(I)-monophosphine and -diphosphine complexes act is in mitochondria. Here, they cause uncoupling of oxidative phosphorylation alterating the inner mitochondrial membrane permeability to cations and protons with the consequent collapse of mitochondrial membrane potential ($\Delta\psi_{mt}$).[9-13] The antitumor activity may be due to loss of $\Delta\psi_{mt}$, which results in decreased ATP synthesis and release of apoptogenic factors from the mitochondria into the cytosol, leading to cell death.[14-15] Considerable interest in the design and development of drugs that specifically compromise the structural and functional integrity of mitochondria is growing.[16-18]

With the aim to potentially increase antitumor activity through synergistic effects, the gold(I) complex [Au(DPPP)(PPh_3)Cl], containing both mono- and di-phosphine ligands, was recently synthesized. It showed appreciable *in vitro* antiproliferative activity against the National Cancer Institute (NCI) 60-cell-line panel derived from tumors of different histotypes; melanoma was the most sensitive subgroup analyzed[19] and thus we focus on this tumor type. Such selectivity has been recently confirmed on additional human melanoma cell lines (JR8, SK-Mel-5, Mel-501, 2/60, 2/21 and GRIG) and the cytotoxic activity resulted higher than or comparable to that of cisplatin.[20]Additionally, apoptotic response of JR8 and 2/60 cells exposed to

[Au(DPPP)(PPh_3)Cl] showed a dose-dependent loss of mitochondrial membrane potential, release of cytochrome *c* and Smac/DIABLO from the mitochondria into the cytosol and a dose-dependent increase in apoptotic cells.[20] Activity of gold complexes with chelating ligands $PPh_2(CH_2)_nPPh_2$ is higher for n = 2, 3 and therefore we attempted to synthesize the analogous mixed phosphine compound [Au(DIPHOS)(PPh_3)Cl], i.e. a complex containing a -$[(CH)_2]_2$- link instead of -$[(CH)_2]_3$- between the 2 PPh_2 units, to test its influence on biological activity. We obtained an unexpected gold-DIPHOS species and below we describe the antiproliferative effect of this novel compound on 3 human melanoma cell lines, JR8, SK-Mel-5 and 2/60. We also include additional studies in solution using NMR and ESI-MS spectroscopy and outline differences between [Au(DPPP)($PPh)_3$Cl] and the gold-DIPHOS complexes, including the novel gold species $[Au_2(DPPP)_2Cl]^+$, studied with DFT. An additional *in vitro* study was performed for both metal compounds on a murine melanoma *in vitro* cell line (B16V) derived from the *in vivo* transplanted B16 melanoma.

RESULTS

Diffraction Study of [{AuCl(PPh_3)}$_2$(μ_2-DIPHOS)].

The X-ray crystal structure of [{PPh_3AuCl}$_2$(μ_2-DIPHOS)] is depicted in Figure 1 and shows a non-chelating DIPHOS ligand bridging 2 gold centers. A solvent chloroform molecule is included in the lattice and does not show chemical interactions with [{AuCl(PPh_3)}$_2$(μ_2-DIPHOS)]. Therefore, the gold center is 3-coordinate, i.e., bound to one Cl and 2 P atoms, one from PPh_3 and one from DIPHOS, and its coordination polyhedron is triangular. Table 1 lists selected structural features both for X-ray and DFT methods, which are described later.

A literature search for Au-DIPHOS chelate, with 3-coordinate metal, shows only 3 compounds in the Cambridge crystallographic database, whereas for DIPHOS bridged gold species, with at least one gold atom 3-coordinate, there are 13 crystal structures. Therefore, having a non-chelate 3-coordinate gold(I)-DIPHOS compound appears statistically favored. Most of these molecules have ring-like connectivity

and the gold coordination geometry is T-shaped, although sometimes ring constraints induce distortions; all have less triangular character than [{AuCl(PPh_3)}$_2$(μ_2-DIPHOS)]. Nine out of the 13 compounds show interactions between both gold atoms as well. The most direct comparison is made with the only Cl derivative, μ_2-2,3-bis(diphenylphosphino)-1,3-butadiene-P,P')-dichloro-digold(I),[21] which has T-shaped gold geometry with Au-Cl bond length of 2.30 Å and 2 Au-P about 2.24 Å. The gold coordination sphere of [{AuCl(PPh_3)}$_2$(μ_2-DIPHOS)], besides differing because it is triangular, has weaker Au-P bonds (2.313(4) Å to PPh_3 and 2.323(4) Å to DIPHOS). This suggests a poor gold protecting capacity by DIPHOS in [{AuCl(PPh_3)}$_2$(μ_2-DIPHOS)], which is confirmed because most Au-P(DIPHOS) bond lengths in the 13 structures mentioned above are generally much shorter, see Figure 2.

Chemistry

Crystalline [{AuCl(PPh_3)}$_2$(μ_2-DIPHOS)] was obtained by mixing in 1:1 molar ratio chloroform solutions of chlorotriphenylphosphinegold(I), [Au(PPh_3)Cl], and DIPHOS. In contrast, an equivalent process using DPPP in dichloromethane instead of DIPHOS, yielded [Au(DPPP)(PPh_3)Cl] as previously described.[19] [{AuCl(PPh_3)}$_2$(μ_2-DIPHOS)] is air- and moisture-stable and has been fully characterized by spectroscopic methods (IR, NMR and ESI MS). Its IR spectrum shows the bands due to the phosphine ligands to be close to those of analogous phosphine gold(I) complexes.[22-23]A weak band at ca. 320 cm^{-1} likely corresponds to ν(Au-Cl) vibration.[23-25] Its $^{31}P\{^1H\}$ NMR spectrum, recorded at room temperature in $CDCl_3$, shows three signals that can be assigned to different phosphorus environments. In the ESI-MS spectrum signals are associated with ionic species and it is only with this technique that we could observe the formation of a species, $[Au(DIPHOS)(PPh_3)]^+$, closely related to the one originally wanted. The reaction between [Au(PPh_3)Cl] and DIPHOS in acetonitrile was monitored with the same technique: When excess DIPHOS was employed, $[Au(DIPHOS)_2]^+$ was the only cation detected in solution; when using equimolar quantities two cations, $[Au(PPh_3)_2]^+$ and $[Au(DIPHOS)_2]^+$, were found to coexist and with an excess of [Au(PPh_3)Cl], the signals due to $[(PPh_3)(DIPHOS)Au]^+$,

$[(PPh_3)(DIPHOS)Au_2Cl]^+$ and $[(PPh_3)_2(DIPHOS)Au_2Cl]^+$ appeared, the latter increasing with the increase in $[Au(PPh_3)Cl]$ concentration.

The $^{31}P\{1H\}$ NMR spectrum of $[Au(DPPP)(PPh_3)Cl]$, in $CDCl_3$ and DMSO, showed the existence of the following products: $[Au(DPPP)(PPh_3)Cl]$, $[Au(DPPP)_2]Cl$, PPh_3, $[Au(PPh_3)_2Cl]$, whereas ESI-MS spectroscopy in MeCN indicated these cations: $[Au(DPPP)PPh_3]^+$, $[Au(DPPP)_2]^+$, $[Au(PPh_3)_2]^+$ and $[Au_2(DPPP)_2]Cl^+$, all of them known except the last one. Therefore, results of ESI-MS and NMR spectra demonstrate that $[Au(DPPP)(PPh_3)Cl]$ undergoes partial dissociation in $CHCl_3$, DMSO and acetonitrile to give stable and known species, many of them carrying DPPP, and the novel cationic species $[Au_2(DPPP)_2]Cl^+$, described later with DFT methods, see Scheme 2.

Since recent studies showed that endogenous hypochlorite interacts with gold(I) anti-arthritic drugs[26] we analyzed the hypochlorite oxidation of $[Au(DPPP)(PPh)_3Cl]$ to Au(III) and found formation of several Au(III) species. First, we analyzed $[Au(DPPP)(PPh_3)Cl]$ by ^1H and $^{31}P\{^1H\}$NMR in water/DMSO solution buffered at physiological pH. Its dissociation toward $[Au(DPPP)_2]Cl$ and $[Au(PPh_3)_2Cl]$ depends on dilution and temperature. Signals due to $[Au(DPPP)(PPh_3)Cl]$, $[Au(DPPP)_2]Cl$ and $[Au(PPh_3)_2Cl]$ are always present. When NaOD was added to the mixture, signals due to PPh_3O and $DPPPO_2$ were immediately observed. On the other hand ^{31}P NMR spectra ($CDCl_3$) of equimolar $[Au(DPPP)(PPh_3)Cl]$ and DCl indicate that $[Au(DPPP)(PPh_3)Cl]$ persists at low pH values, and the equilibrium shown in Scheme 3 is shifted to the right.

When ClO^- was added to a NMR test-tube containing a $CDCl_3$ solution of $[Au(DPPP)(PPh_3)Cl]$, several signals appeared immediately. Some were assigned to the following species: $[PPh_3AuCl_3]$,[27] $[(DPPP)AuCl_2]Cl$, $[(PPh_3)AuCl]$, $[(DPPP)AuCl]$, $[Au(DPPP)_2]Cl$. It is worth noting that upon ClO^- addition the solution becomes yellow and $[AuCl_4]^-$ was identified by UV spectroscopy.[28]

Acetonitrile/H_2O solutions of [Au(DPPP)(PPh_3)Cl] and ClO^- have been also investigated by ESI MS spectroscopy. $[AuCl_4]^-$ and $[AuCl_2]^-$ in 5:1 ratio have been identified in the negative spectrum, whereas in the positive one, signals due to $[(PPh_3O)_2 + Na]^+$, $[(DPPPO_2)_2 + Na]^+$, $[(PPh_3O)(DPPPO_2) + Na]^+$ $[PPh_3AuCl_2]^+$, $[(DPPP)AuCl_2]^+$, $[(PPh_3)_2Au]^+$, $[(DPPP)(PPh_3)Au]^+$ and $[(DPPP)Au(Cl)(H_2O)]^{++}$ are present depending on dilution of solution. Upon further addition of ClO^-, the signals due to $[(PPh_3)_2Au]^+$, $[(DPPP)(PPh_3)Au]^+$ disappear, whereas those due to $[(PPh_3O)_2 + Na]^+$, $[(DPPPO_2)_2 + Na]^+$, $[PPh_3AuCl_2]^+$, and $[(DPPP)AuCl_2]^+$ increase in intensity. When large excess ClO^- is added, signals due to $[PPh_3AuCl_2]^+$ and $[(DPPP)AuCl_2]^+$ also disappear and the only one present for gold containing species is due to $[AuCl_4]^-$. By adding PPh_3 or DPPP to this solution, $[PPh_3AuCl_2]^+$, and $[(DPPP)AuCl_2]^+$ form again. Finally addition of strong excess of PPh_3 regenerates PPh_3AuCl, as expected.[28] Spectroscopic data therefore suggest that reacting [Au(DPPP)(PPh_3)Cl] with ClO^- oxidizes gold(I) to gold(III), as confirmed by the presence of several gold(III)-phosphine cations and $[AuCl_4]^-$ in the ESI MS spectrum. This is also supported by the fact that addition of an equimolar quantity of PPh_3 to the above NMR solution produces PPh_3AuCl_3. The oxidation of gold(I) to gold(III) is accompanied by the oxidation of both phosphine donors to phosphinooxide species.

In conclusion, ^{31}P NMR spectra of chloroform (or D_2O/DMSO) solutions containing [Au(DPPP)(PPh_3)Cl] and ClO^- agree with ESI MS spectra of acetonitrile solution containing the same species; these are input for DFT calculations also described later.

Cytotoxic activity

The *in vitro* cytotoxic activity of the gold complex [{AuCl(PPh_3)}$_2$(μ_2-DIPHOS)] was investigated in JR8, SK-Mel-5 and 2/60 human melanoma cell lines exposed to different concentrations (from 0.1 to 1000 μM) for 48 h. A dose-dependent inhibition of cell growth was observed in all cell lines (Figure 3), with IC_{50} values ranging from 2.7 to 28 μM. This cytotoxic effect was compared to that reported for [Au(DPPP)(PPh_3)Cl],[20] under the same experimental conditions (Table 2): the DIPHOS complex was less potent than the DPPP one in inhibiting cell

growth. A related study was performed on the B16V murine melanoma cell line for both [Au(DPPP)(PPh_3)Cl] and [{AuCl(PPh_3)}$_2$(μ_2-DIPHOS)]. The dose-response curves obtained for the two compounds are depicted in Figure 4; non linear regression analysis gave IC_{50} values of 0.09 ± 0.02 μM and 0.32 ± 0.08 μM, respectively (mean ± SD of 4 independent experiments). The difference between the two values is highly statistically significant by Student's *t* test for independent samples ($p < 0.001$).

Theoretical calculations

The structural features of $[Au_2(DPPP)_2Cl]^+$ were investigated with DFT. Initial coordinates for a non-chelate arrangement (Scheme 4, left) were obtained after modification of the closely related bis(μ_2-chloro)-bis(μ_2-R,S-(1-diphenylphosphinobut-2-yl)-diphenylphosphinite)-di-gold(I) crystal structure,[29] see Figure 5. In addition, an alternative connectivity having two chelating "Au(DPPP)" moieties linked by the bridging Cl atom was explored (Scheme 4, right). The molecule having the lowest energy showed a Au-Cl-Au moiety typical of aurophilic interaction and is shown in Figure 6. [{PPh_2AuCl}$_2$(μ_2-DIPHOS)] was investigated with DFT technique because anisotropic crystalline decay was seen during data collection. Initial coordinates from the X-ray structure were geometry minimized and the triangular coordination resulted more regular.

To study the reactivity of ClO^- towards [Au(DPPP)(PPh_3)Cl] we decreased calculation time by replacing all Ph groups with methyls in phosphine ligands so that [Au(DPPP)(PPh_3)Cl] was modeled as [Au(DMPP)($PMet_3$)Cl]. When comparing the calculated structures of [Au(DMPP)($PMet_3$)Cl] and its cationic derivative $[Au(DMPP)(PMet_3)]^+$ it is seen that the role of Cl^- is almost insignificant from a structural viewpoint, as the distance between the Au and the plane made by the 3 P atoms is 0.280 Å and 0.016 Å, respectively: that is, both complexes can be considered as 3-coordinate. Since $[Au(DPPP)(PPh_3)]^+$ is observed experimentally with NMR and ESI-MS, and its solubility is higher than [Au(DPPP)($PPh)_3$Cl] in biological fluids, we suggest that this cationic species may be the active drug

and so we modeled the redox process using $[Au(DMPP)(PMet_3)]^+$ as starting material (see Scheme 5). ΔG for this reaction is -126.7 kcal/mol and indicates thermodynamic feasibility.

DISCUSSION

Melanoma is the most aggressive of skin tumors, and disseminated disease is characterized by a very poor clinical outcome, not modified by conventional anticancer treatments.[30] New agents and novel approaches are under preclinical evaluation for this malignancy.[31] In this context, it has been shown that $[Au(DPPP)(PPh_3)Cl]$ is highly cytotoxic against several human tumor cell lines and displays a selective activity in melanoma cells.[19] This activity has been recently confirmed on other human tumor cells, and demonstrated to be related to apoptosis induction associated with impairment of mitochondrial function.[20]

The aim of the present study was to assess on the cytotoxicity the effect of shortening the bridge between PPh_2 units, that is modifying $-[(CH)_2]_3-$ to $-[(CH)_2]_2-$. The rationale for this synthesis was also supported by the fact that less lipophilic phosphines are more tumor-selective and induce fewer side effects in their gold chelates.[32]

Applying the same synthetic route[19] used for $[Au(DPPP)(PPh_3)Cl]$ gave crystalline $[\{AuCl(PPh_3)\}_2(\mu_2\text{-DIPHOS})]$ as proven by diffraction methods; this compound was chemically characterized with IR, NMR, ESI-MS spectroscopy and elemental analyses. The X-ray crystal structure of $[\{AuCl(PPh_3)\}_2(\mu_2\text{-DIPHOS})]$ shows a non-chelating DIPHOS ligand as it links 2 gold centers. Therefore, the metal is 3-coordinate, i.e., bound to one Cl and 2 P atoms, one from PPh_3 and one from DIPHOS. Considering that a) DIPHOS induces a lower bite angle than DPPP and b) the tendency of gold(I) to stabilize low coordination numbers (2 or 3 are more preferred than 4), we suggest that in combination the formation of a non chelating species is induced; this is statistically favored as seen in the literature (Figure 2).

In JR8, SK-MEL-5 and the melanoma clone 2/60 cell lines the *in vitro* cytotoxicity of [{AuCl(PPh_3)}$_2$(μ_2-DIPHOS)] shows higher IC_{50} values (1.5 times or more) than those reported for [Au(DPPP)(PPh_3)Cl].[20] Therefore, we performed a comparative study in solution for both species to determine a possible explanation for the systematic difference in activity. Since [Au(DPPP)(PPh_3)Cl] undergoes partial dissociation in solution to several compounds including the cytotoxic agent $[Au(DPPP)_2]^+$, the resulting variety may help increasing the possibility of transporting DPPP to the target, (scheme 2). One of these compounds is the novel cationic species $[Au_2(DPPP)_2Cl]^+$, whose equivalent was not detected for [{AuCl(PPh_3)}$_2$(μ_2-DIPHOS)]. Its structural features were investigated with DFT methods that gave the following observations: (1) a non chelating connectivity having a Cl-bridged structure (Figure 5); (2) an alternative connectivity having two "Au(DPPP)$_2$" chelate moieties bridged by the Cl atom, depicted in Figure 6, with an Au—Au separation of 2.711 Å thus showing a stronger aurophilic interaction compared to related crystalline compounds having the same Au-Cl-Au moiety.

Therefore, by shortening the distance between both PPh_2 groups (using DIPHOS instead of DPPP) a different gold complex is stabilized: having a unique triangular gold coordination and a non-chelating structure with weaker Au-P bonds than related non-chelate Au-DIPHOS compounds. Since a chelating ligand establishes stronger metal binding than a non-chelating one, the latter complex is less stable possibly explaining the lower activity than that observed for [Au(DPPP)(PPh_3)Cl]. This structure-activity relationship suggests a straightforward test on the crystal structures of other potential gold(I)-diphosphines: a strong Au-P binding favors diphosphine metal protection and increases access to the target. To check this hypothesis we performed additional tests for both gold compounds on the B16V murine melanoma cell line. From dose-response curves following 48h exposure to [Au(DPPP)(PPh_3)Cl] and [{AuCl(PPh_3)}$_2$(μ_2-DIPHOS)] IC_{50} values of 0.09 and 0.32 μM, respectively, were obtained. These results confirm that the non-chelate complex [{AuCl(PPh_3)}$_2$(μ_2-DIPHOS)] has weaker activity than the

chelate complex [Au(DPPP)(PPh_3)Cl]. The activity of both complexes in the B16V panel is about 10 times higher than in JR8, SK-MEL-5 and 2/60 cell lines.

The mechanism of action of gold(I)-diphosphines derivatives is still largely unknown. Gold seems to function as a carrier for the diphosphine ligand which can be displaced, for example, by thiol groups reacting with gold(I). The resulting free diphospines are able to function as antiproliferative agents.[33-35] However, a more direct involvement of gold in antitumor activity is feasible, as some gold(III) compounds, without any phosphine bound to the metal, are also active against several tumor models.[36] Potential explanations may come from clinically used anti-arthritic Au(I) drugs as they do not cause the release of peptide from human leukocyte antigen (HLA-DR1) *in vitro* but the Au(III) square-planar compound K[$AuCl_4$] releases peptides from HLA-DR4,[37] which are frequently found in individuals with rheumatoid arthritis; these features were also analyzed for other isoelectronic square-planar complexes (cisplatin and $K_2[PdCl_4]$). Oxidation of Au(I) to Au(III) has been reported *in vivo*[38] and *in vitro*[39] and Au(III) metabolites formed *in vivo* are responsible for severe allergic side effects from gold therapy. In addition, Au(I) pharmaceuticals are considered pro-drugs that convert to Au(III) after interaction with hypochlorite produced by phagocytes.[26] Using spectroscopic NMR and ESI MS of solution chemistry we show that upon addition of hypochlorite to [Au(DPPP)(PPh_3)Cl] there is oxidation to $[AuCl_4]^-$, $DPPPO_2$ and PPh_3O. A DFT investigation that includes structural calculations of these compounds finds a related oxidation reaction having thermodynamic feasibility.

CONCLUSIONS

The confirmation of chelating diphosphines as a necessary feature for effective antitumor activity in their gold(I) derivatives is shown by [Au(DPPP)(PPh_3)Cl] being more effective than [{AuCl(PPh_3)}$_2$(μ_2-DIPHOS)] against melanoma. [Au(DPPP)(PPh_3)Cl] decomposition in solution includes the novel cation $[Au_2(DPPP)_2Cl]^+$ whose biological role is not clear at present. In addition, redox interaction of [Au(DPPP)(PPh_3)Cl] with the endogenous hypochlorite anion leads

to the corresponding square-planar $[AuCl_4]^-$ and phosphine oxidation; DFT shows this reaction to be thermodynamically favorable and perhaps related to the antitumor mechanism of action.

Experimental Section

Chemistry

DIPHOS, DPPP and $(PPh_3)AuCl$ were purchased from Aldrich and used without further purification. All solvents were dried, degassed, and distilled prior to use. Elemental analyses (C, H) were performed with a Fisons Instruments 1108 CHNS-O Elemental analyzer. Buffer solution (Fluka) pH 9.0 (20.0°C) Sodium tetraborate (borax/hydrochloricacid); pH 5.0 (20°C) sodium citrate. IR spectra were recorded from 4000 to 100 cm^{-1} with a Perkin-Elmer System 2000 FTIR instrument. ^1H and $^{31}P\{^1H\}$ NMR spectra, referenced to $Si(CH_3)_4$ and external 85% H_3PO_4 respectively, were recorded on a VXR-300 Varian spectrometer (300 MHz for ^1H, and 121.4 MHz for ^{31}P). Relative intensity of signals is given in square brackets and *J* in hertz. The interaction of $[Au(DPPP)(PPh_3)Cl]$ with hypochlorite was studied with ^1H and ^{31}PNMR spectra recorded on a Mercury Plus Varian 400 NMR spectrometer (400 MHz for ^1H, and 162.1 MHz for ^{31}P). Positive and negative electrospray mass spectra were obtained with a Series 1100 MSI detector HP spectrometer, using an acetonitrile mobile phase. Solutions (3 mg/mL) for electrospray ionization mass spectrometry (ESI-MS) were prepared using reagent grade acetonitrile. For the ESI-MS data, masses and intensities were compared to those calculated by using the IsoPro Isotopic Abundance Simulator, version 2.1;[40] peaks containing chloride are identified as the centres of isotopic clusters.

Chloro-triphenylphosphine-1,3-bis(diphenylphosphino)propane-gold(I), $[Au(DPPP)(PPh_3)Cl]$, was synthesized as previously reported.[19] IR (Nujol mull, cm^{-1}): 3060w, 3039w, 1990w, 1906w, 1826w, 1770w, 1671w, 1582m, 1569m, 1436m, 1313m, 1196br, 1094s, 1070w, 1043w, 1026w, 998w, 971m, 824m, 794m, 761m, 747m, 738m, 722m, 710m, 697s, 648m, 617w, 547m, 530m, 515s, 508s, 491m, 470m, 429m, 398w, 357w, 329w, 302w, 280w, 252sh, 248w, 227w. ^1H NMR ($CDCl_3$, 295 K, δ ppm): 2.2 br (CH_2, 2H), 2.6br (CH_2, 4H), 7.0-7.7m br (CHPh, 35H). ^{31}P NMR (DMSO, 293K, δ ppm): 0.11br

[10], 26.6br [1], 31.0 [2], 31.7br [10], 34.62br [30]. ^{31}P NMR (CDCl3, 293K, δ ppm): -1.7br [1], 26.4br [1], 32.7br [1].

The ^{31}P{1H} NMR spectrum of [Au(DPPP)(PPh_3)Cl], taken at room temperature in $CDCl_3$, shows 3 signals that can be assigned to the two different phosphorus environments in the complex (PPh_3 and DPPP) and to [Au(DPPP)$_2$]Cl. Some minor signals appear after 30 min due to free PPh_3 and [Au(PPh_3)$_2$Cl], suggesting partial dissociation of the complex in this solvent. A similar behavior has been displayed in DMSO where the predominant species are [Au(DPPP)$_2$]Cl, [Au(DPPP)PPh_3Cl] and [Au(PPh_3)$_2$Cl] respectively.

To confirm the dissociation equilibrium in solution of [Au(DPPP)(PPh_3)Cl] an electron spray ionization mass spectrometry (ESI-MS) study was carried out on its MeCN solutions at different concentrations. In the positive mode the following cations were identified: [Au(DPPP)(PPh_3)]$^+$, [Au(DPPP)$_2$]$^+$, [Au(PPh_3)$_2$]$^+$ and [Au$_2$(DPPP)$_2$]Cl$^+$, with the latter 3 species being less abundant.

ESI-MS (MeCN): + 721.5 [10] [(PPh_3)$_2$AuCl]$^+$, 871.7 [80] [Au(DPPP)(PPh_3)]$^+$, 1021.8 [100] [Au(DPPP)$_2$]$^+$, 1253.8 [5] [Au$_2$(DPPP)$_2$]Cl]$^+$. Therefore, by combining ESI-MS and NMR spectra it is demonstrated that this compound undergoes partial dissociation in $CHCl_3$, DMSO and MeCN yielding stable and known species plus the novel cationic species [Au$_2$(DPPP)$_2$]Cl$^+$.

Interaction of [Au(DPPP)(PPh_3)Cl] with hypochlorite. ^{31}P NMR ($CDCl_3$, 293K, δ ppm): 16.5s [10], 27.8s [2], 28.2s [1], 29.2 [2], 30.6 [10], 33.5d [2] (82Hz), 34.1 [5], 34.2 [10], 41.1d [2] (44Hz), 41.9 [2], 45.0 [2]. ^{1}H NMR (CD_2Cl_2, 293K, δ ppm): 1.9 br (2H, CH_{2DPPP}), 1.9 br (2H, CH_{2DPPP}), 2.7 br (4H, CH_{2DPPP}), 7.0-8.0 (35H, $CH_{PPh3 + DPPP}$)

ESI MS (MeCN, 25 °C): (–) 338.8 [100] ($AuCl_4^-$), 266.9 [40] ($AuCl_2^-$). (+) 911 [100] (($DPPPO_2$)$_2$ + Na$^+$), 745 [40] [(PPh_3O)($DPPPO_2$) + Na]$^+$, 679 [65] [(DPPP)$AuCl_2$]$^+$, 529 [25] [(PPh_3)$AuCl_2$]$^+$, 445 [80] [($DPPPO_2$) + H]$^+$.

Bis(chloro-triphenylphosphinegold(I))-μ2-1,2-bis(diphenylphosphino)ethane. Since crystalline [Au(DPPP)(PPh_3)Cl] was obtained from slow evaporation of [Au(PPh_3)Cl] and DPPP in

dichloromethane (1:1 ratio),[19] we mixed [Au(PPh_3)Cl] and DIPHOS accordingly. Crystalline material from chloroform solutions was obtained and, unexpectedly, diffraction methods showed it to be [{AuCl(PPh_3)}$_2$(μ_2-DIPHOS)]. When trying the same 1:1 ratio in diethyl ether, $[(DIPHOS)_2Au]^+$ formed, that is a different product than obtained from chloroform. However, reacting [Au(PPh_3)Cl] and DIPHOS (2:1) in diethyl ether yielded [{AuCl(PPh_3)}$_2$(μ_2-DIPHOS)], as reported above for chloroform. That is, upon addition of 0.41 g of DIPHOS (ca 1.0 mmol) to a suspension (50 mL) of [Au(PPh_3)Cl] (1.00 g, ca. 2.0 mmol) in diethyl ether, a colorless precipitate formed. The suspension was then stirred for 4 h and filtered and the precipitate washed with diethyl ether (20 mL) to give 0.70 g (0.5 mmol, 50%) of the title compound, mp 189-191 °C. Anal. ($C_{62}H_{54}Au_2Cl_2P_4$) C, H. IR (Nujol mull, cm^{-1}): 3050w, 3020w, 1585w, 1572w, 545m, 532m, 515s, 508s, 492s, 454m. ^{1}H NMR ($CDCl_3$): δ 2.5 (br, 2H, CH_2), 3.0 (br, 2H, CH_2), 7.2-7.8 (m, 50H, C_6H_5). ^{31}P NMR ($CDCl_3$): 21.14, 33.35, 34.55. ESI MS (+) (CH_3CN): 721.5 (30) [$(PPh_3)_2Au^+$], 857.5 (40) [(PPh_3)(DIPHOS)Au^+], 993.8 (100) [$(DIPHOS)_2Au^+$], 1090 (20) [(PPh_3)(DIPHOS)Au_2Cl^+], 1352 (10) [$(PPh_3)_2$(DIPHOS)Au_2Cl^+], 1457 (5) [$(DIPHOS)_2Au_3Cl_2^+$]. When different molar ratios were employed, for example Au(PPh_3)Cl : DIPHOS (1:1) or Au(P(Ph_3)Cl : DIPHOS (1:2), the well-known [Au $(DIPHOS)_2$]Cl formed.

X-ray Study of [{AuCl(PPh_3)}$_2$(μ_2-DIPHOS)].

Very slow evaporation of this compound in chloroform solution afforded plate shaped crystals. A preliminary Weissenberg study showed cell parameters and space group. Crystal was placed in a quartz capillary to attenuate the strong and anisotropic decay. The molecular structure was determined with the Patterson function and successive Fourier localizations using CAOS program.[41] The obtained high R_f is probably due to anisotropic crystal decay. The molecule is centro-symmetric with the inversion center located half way along the ethylene bridge. The asymmetric unit is half a molecule plus $CHCl_3$ so that the crystalline compound is formally [{AuCl(PPh_3)}$_2$(μ_2-DIPHOS)] · 2 $CHCl_3$. Table S4 shows crystallographic data.

Theoretical Study

The structural features of the novel cationic species $[Au_2(DPPP)_2Cl]^+$ were analyzed with density functional theory (DFT) using the Accelrys program Cerius2 4.6, subroutine DMol3 on an Octane SGI computer.[42] Reliability of this program was already observed in performing structural calculations on related compounds.[43] Due to the large scale calculations, an electron core potential (ECP) technique was employed. Local density was the Perdew and Wang (PWC) functional[44] using a double numeric basis set with polarization functions (DNP)[45] on all atoms. Initial coordinates for a non-chelate arrangement of $[Au_2(DPPP)_2Cl]^+$ (Scheme 4, left) were obtained after modification of the closely related bis(μ_2-chloro)-bis(μ_2-R,S-(1-diphenylphosphinobut-2-yl)-diphenylphosphinite)-di-gold(I) crystal structure,[29] which possesses 2 Cl atoms bridging the 2 metal centers, and a C-C-O link between the 2 PPh_2 moieties. Therefore, this link was updated to $-(CH_2)_3-$and one Cl atom was excluded. To ensure obtaining an absolute energy minimum, discrete modifications of the initial structure were performed; all of them converged to the same geometry, see Figure 5. The Au-Au separation of 4.441Å is slightly longer than the one from which the structure was modeled (4.338 Å). Cartesian coordinates of the converged structure are deposited in Supporting Information Available (Table S1). Gold(I) shows marked preference for coordination number 2 and an alternative configuration without the Cl bridge was also explored. In this arrangement one gold is 3-coordinate, bound to Cl and 2 P atoms, and the other gold is 2-coordinate, bound to 2 P atoms. Several models of this type did not reach convergence and their minimization paths became erratic. Also, resulting structures using these pathways showed energy markedly higher than the bridged structure and we conclude that the Au-Cl-Au bridged cation is preferred to the one having a terminal Cl.

An alternative connectivity having two chelating "Au(DPPP)" moieties linked by a Cl atom was also explored (Scheme 4, right). The coordinates of the flexible tri-methylene bridge and the phenyls were widely varied to avoid trapping in non absolute minima. The best converged molecule possesses a Au-Cl-Au moiety typical of aurophilic interaction and is shown in Figure 6; related coordinates are also

deposited in Supporting Information Available (Table S2). The same DMol3 conditions were used to refine the molecular structure of the crystalline [{AuCl(PPh_3)}$_2$(μ_2-DIPHOS)] species.

Calculations for oxidation of [Au(DPPP)(PPh_3)Cl] to $[AuCl_4]^-$, PPh_3O and $DPPPO_2$ were performed using DMol3 as implemented in the program Materials Studio 4.0 (PC version) using a BP/DNP basis set closely related to that used in the SGI platform, and including relativistic effects for the metal.

Biological Study

Cell lines

Human melanoma cell lines, JR8, SK-MEL-5 and the melanoma clone 2/60 (selected from the human melanoma cell line 665/2 by micromanipulation in soft agar), were used to compare with related data.[20] The biological characteristics of JR8, SK-MEL-5, and 2/60 have been previously described.[46-47] Cell lines were maintained in logarithmic growth phase at 37°C in a 5% CO_2 humidified atmosphere in air. RPMI-1640 medium (Biowhittaker, Verviers Industries, Kibbutz Beth Haemek, Israel), containing 10% fetal calf serum, 2 mM L-glutamine and 0.1 mg/ml gentamycin was used for all cell lines. For these cell lines the experiments were performed within 10 passages from thawing. An additional test *in vitro* was performed for both compounds in the B16V cell line. This murine model, an *in vitro* line derived from the *in vivo* transplanted B16 melanoma, was a gift from Dr. R. Supino (Istituto Nazionale Tumori, Milan, Italy).[48] Cells were maintained in RPMI-1640 medium (Sigma-Aldrich, Milan, Italy), supplemented with 10% fetal bovine serum (Celbio, Italy), 2 mM glutamine, 1% antibiotic mixture and 0.03 mM $K_3Fe(CN)_6$ at 37°C in a humidified 5% CO_2 atmosphere.

Drugs

[{AuCl(PPh_3)}$_2$(μ_2-DIPHOS)] was reconstituted in sterile DMSO at a concentration of 5 mM and then diluted with sterile water to the desired concentrations, immediately before each experiment, for JR8, SK-MEL-5, the melanoma clone 2/60 and B16V cell lines. The same technique was applied for [Au(DPPP)(PPh_3)Cl] in the B16V cell line.

Cell survival assay

The sulforhodamine B (SRB) assay was performed on all the cell lines tested as described[49] with minor modifications. Briefly, according to the growth profiles previously defined for each cell line, adequate numbers of cells in 0.2 ml culture medium were plated in each well of a 96-well plate and allowed to attach for 24 h. Cells were exposed at 37°C for 48 h to different concentrations of the two gold complexes ranging between 0.1-1000 μM for the human melanoma cell lines or between 0.01-10 μM for B16V cells. Each experiment included eight replications for each concentration tested; control samples were run with 0.2% DMSO. At the end the 48 h period of incubation with the gold complexes, cells were fixed and processed for SRB staining. The optical density (OD) was read at 550 nm using a Universal Microplate Reader EL800 (Bio-Tek Instruments) and the results were expressed as cell growth obtained from the ratio of the absorbance values of gold complex-treated samples and those of controls. Dose-response curves were analyzed by nonlinear regression analysis and IC_{50} values were estimated using GraphPad Prism software, v. 4.03. The *in vitro* activity of the drugs was expressed as IC_{50} (*i.e.* the concentration inhibiting cell proliferation by 50%).

REFERENCES:

1. Zhang, C. X.; Lippard, S. J. New metal complexes as potential therapeutics. *Current Opinion Chem. Biol.* **2003**, *7*, 481-489.
2. Guo, Z.; Sadler, P. J. Medicinal inorganic chemistry. A*dv. Inorg. Chem.* **2000**, *49*, 183-306.
3. Shaw, C. F. III. Gold-based therapeutic agents. *Chem. Rev.* **1999**, *99*, 2589-2600.
4. Tiekink, E. R. T. Gold derivatives for the treatment of cancer. *Crit. Rev. Oncol. Hematol.* **2002**, *42*, 225-248.

5. Simon, T. M.; Kunishima D. H.; Vibert, G. J.; Lorber, A. Screening Trial with the coordinated gold compound auranofin using mouse lymphocytic leukemia P388. *Cancer Res.* **1981**, *41*, 94-97.

6. Mirabelli, C. K.; Johnson, R. K; Sung, C. -M.; Faucette, L. F.; Muirheard, K.; Crooke, S. T. Evaluation of the *in vivo* antitumor activity and *in vitro* cytotoxic properties of Auranofin, a coordinated gold coumpound, in murine tumor models. *Cancer Res.* **1985**, *45*, 32-39.

7. Mirabelli, C. K.; Johnson, R. K.; Hill, D. T.; Faucette, L. F.; Girard, G. R.; Kuo, G. Y.; Sung, C. -M.; Crooke, S. T. Correlation of the *in vitro* cytotoxic and *in vivo* antitumor activities of Gold (I) coordination complexes. *J. Med. Chem.* **1986**, *29*, 218-223.

8. Berners-Price, S. J.; Girard, G. R.; Hill, D. T.; Sutton, B. M.; Jarret, P. S.; Faucette, L. F.; Johnson R. K.; Mirabelli, C. K.; Sadler, P. J.; Cytotoxicity and antitumor activity of some tetrahedral bis(diphosphino)gold(I) chelates. *J. Med. Chem.* **1990**, *33*, 1386-1392.

9. Rigobello, P.; Messori, L.; Marcon, G.; Cinellu, A. M.; Bragadin, M.; Folda, A.; Scutari, G.; Bindoli, A. Gold complexes inhibit mitochondrial thioredoxin reductase: consequences on mitochondrial functions. *J. Inorg. Biochem.* **2004**, *98*, 1634-1641.

10. Rigobello, M. P.; Scutari, G.; Folda, A.; Bindoli, A. Mitochondrial thioredoxin reductase inhibition by gold(I) compounds and concurrent stimulation of permeability transition and release of cytochrome c. *Biochem. Pharmacol.* **2004**, *67*, 689-696.

11. Hoke, G. D.; Rush, G. F. Mechanism of alterations in isolated rat liver mitochondrial function induced by gold complexes of bidentate phosphines. *J. Biol. Chem.* **1988**, *263*, 11203-11210.

12. Barnard, P. J.; Baker, M. V.; Berners- Price, S. J.; Day, D. A. Mitochondrial permeability transition induced by dinuclear gold(I)-carbene complexes: potential new antimitochondrial antitumour agents. *J. Inorg. Biochem*. **2004**, *98*, 1642-1647.

13. McKeage, M. J. Gold opens mitochondrial pathways to apoptosis. *Br. J. Pharmacol.* **2002**, *136*, 1081-1082.

14. Ly, J. D.; Grubb, D. R.; Lawen, A. The mitochondrial membrane potential (deltapsi(m)) in apoptosis; an update. *Apoptosis* **2003**, *8,* 115-128.

15. Zhou, L. L.; Zhou, L. Y.; Luo, K. Q.; Chang, D. C. Smac/DIABLO and cytochrome c are released from mitochondria through a similar mechanism during UV-induced apoptosis. *Apoptosis* **2005**, *10,* 289-299.

16. Garber, K. Targeting mitochondria emerges as therapeutic strategy. *J. Natl. Cancer Inst.* **2005**, *97*, 1800-1801.

17. Bras, M.; Queenan, B.; Susin, S. A. Programmed cell death via mitochondria: different modes of dying. *Biochemistry,* **2005**, *70*, 231-239.

18. Mohamad, N.; Gutierrez, A.; Nunez, M.; Cocca, C.; Martin, G.; Cricco, G.; Medina, V.; Rivera, E.; Bergoc, R. Mitochondrial apoptotic pathways. *Biocell.* **2005**, *29*, 149-161.

19. Caruso, F.; Rossi, M.; Tanski, J., Pettinari, C.; Marchetti, F. Antitumor activity of the mixed phosphine gold species chlorotriphenylphosphine-1,3-bis(diphenylphosphino)propanegold(I). *J. Med. Chem.* **2003**, *46*, 1737-1742.

20. Caruso, F.; Villa R.; Rossi M.; Pettinari C.; Paduano F.; Pennati M.; Daidone M.G.; Zaffaroni N. Mitochondria are primary targets in apoptosis induced by the mixed phosphine gold species chlorotriphenylphosphine-1,3-bis(diphenylphosphino)propanegold(I) in melanoma cell lines. *Biochem. Pharmacol*. **2006**, *6*, 773-781.

21. Schmidbaur, H.; Dziwok, K.; Grohmann, A.; Mueller, G. Further evidence for attractive interactions between gold(I) centers in binuclear complexes. *Chem. Ber.* **1989**, *122*, 893-895.

22. (a) Elder, R. C.; Zeiher, E. H. K.; Onady, M.; Whittle, R. R. Nearly regular tetrahedral geometry in a gold(I)-phosphine complex. X-ray crystal structure of tetrakis(methyldiphenylphosphine)- gold(I) hexafluorophosphate. *J. Chem. Soc., Chem. Commun.* **1981**, 900-901. (b) Jones, P. G. Is Regular tetrahedral geometry possible in

gold(I)-phosphine complexes? X-ray crystal structure of three modifications of $[(PPh_3)_4Au][BPh_4]$ *J. Chem. Soc., Chem. Commun.* **1980**, 1031-1033. (c) Parish, R. V.; Rush, J. D. Gold-197 Mössbauer spectra of two-, three, and fourcoordinate gold(I) complexes. *Chem. Phys. Lett.* **1979**, *63,* 37-39. (d) Mays, M. J.; Vergnano, P. A. Structure and bonding in gold(I) compounds. A phosphorus-31 nuclear magnetic study of the structure of some gold(I) phosphine complexes in solution. *J. Chem. Soc., Dalton Trans.* **1979**, 1112-1115. (e) Colburn, C. B.; Hill, W. E.; McAuliffe, C. A. ^{31}P NMR study of tertiary phosphine complexes of gold(I). *J. Chem. Soc., Chem. Commun.* **1979**, 218-219. (f) Parish, R. V.; Parry, O.; McAuliffe, C. A. Characterization of two-, three, and four-coordinate gold-(I) complexes by 197Au Mo¨ssbauer and ^{31}P-$\{^1H\}$ nuclear magnetic resonance spectroscopy. *J. Chem. Soc., Dalton Trans.* **1981**, 2098-2104. (g) Muir, J. A.; Muir, M. M.; Arias, S.; Campana, C. F.; Dwight, S. K. Structure of the monoclinic form of thiocyanato tris(triphenylphosphine)gold(I) monohydrate. *Acta Crystallogr.* **1982**, *38B,* 2047-2049. (h) Uson, R.; Laguna, A.; Vicente, J.; Garcia, J.; Jones, P. G.; Sheldrick, G. M. Preparation of three- and four-coordinate gold(I) complexes: crystal structure of bis[*o*-phenylene, bis(dimethylarsine)]gold(I) bis(pentafluorophenyl)aurate(I) *J. Chem. Soc., Dalton Trans.* **1981**, 655-657. (i) Muir, J. A.; Muir, M. M.; Arias, S.; Jones, P. G.; Sheldrick, G. M. The crystal and molecular structure of the orthorhombic form of thiocyanato tris(triphenylphosphine)gold(I) monohydrate $[(Ph_3P)_3Au(SCN)].H_2O$ *Inorg. Chim. Acta* **1984**, *81,* 169-174.

23. (a) Bates, P. A.; Waters, J. M. A tetrahedral complex of gold(I). The crystal and molecular structure of $Au(Ph_2PCH_2CH_2PPh_2)_2$-$Cl.2H_2O$. *Inorg. Chim. Acta* **1984**, *81,* 151-154. (b) Berners-Price, S. J.; Mazid, M. A.; Sadler, P. J. Stable gold(I) complexes with chelate rings: solution studies of bis(phosphino) ethane complexes and X-ray crystal structure of bis[1,2-bis(diphenylphosphino)ethane] gold(I) hexafluoroantimoniate-acetone (1/1). *J. Chem. Soc., Dalton Trans.* **1984**, 969-974. (c) Berners-Price, S. J.; Brevard, C.; Pagelot,

A.; Sadler, P. J. Cu-($Ph_2PCH_2CH_2PEt_2)_2Cl$: a chelated copper(I) complex with tetrahedral stereochemistry. Rate of inversion compared with those of isostructural silver(I) and gold(I) complexes. *Inorg. Chem.* **1986**, *25*, 596-599. (d) Berners-Price, S. J.; Sadler, P. J. Gold(I) complexes with bidentate tertiary phosphine ligands: formation of annular vs tetrahedral chelated complexes. *Inorg. Chem.* **1986**, *25*, 3822-3827. (e) Berners-Price, S. J.; Jarret, P. S.; Sadler, P. J. 31P NMR studies of $[Au_2(\mu\text{-dppe})]^{2+}$ antitumor complexes. Conversion into $[Au(dppe)_2]^+$ induced by thiols and blood Plasma. *Inorg. Chem*. **1987**, *26,* 3074-3077.

24. (a) Barranco, E. M.; Crespo, O.; Gimeno, M. C.; Laguna, A.; Jones, P. G.; Ahrens, B. Gold and silver complexes with the ferrocenyl phosphine $FcCH_2PPh_2$ [Fc = (η^5-C_5H_5)Fe(η^5-C_5H_4)]. *Inorg. Chem.* **2000**, *39,* 680-687. (b) Bardajı´, M.; Laguna, A.; Orera, V. M.; Villacampa, M. D. Synthesis, structural characterization, and luminescence studies of gold(I) and gold(III) complexes with a triphosphine ligand. *Inorg. Chem.* **1998**, *37*, 5125-5130. (c) Bardajı`, M.; Laguna, A.; Vicente, J.; Jones, P. G. Synthesis of luminescent gold(I) and gold(III) complexes with a triphosphine ligand. *Inorg. Chem.* **2001**, *40,* 2675-2681.

25. Cooper, M. K.; Mitchell, L. E.; Henrick, K.; McPartlin, M.; Scott, M. The synthesis and X-ray structure analysis of dichloro{1,3-bis(diphenylphosphino)propane}digold(I). *Inorg. Chim. Acta* **1984**,*84,* L9-L10.

26. Babior, B. M.; Kipnes, R. S.; Curnutte, J. T. Biological defense mechanisms. The production by leukocytes of superoxide, a potential bactericidal agent. *J. Clin. Invest.* **1973**, *52*, 741–744.

27. Attar, S.; Nelson, J. H.; Bearden, W. H.; Alcock, N. W.; Solujic, L.; Milosavljevic, E. B. Phosphole complexes of gold(III) halides: Synthesis, structure, electrochemistry and ligand redistribution reactions. *Polyhedron* **1991**, *10*, 1939-1949.

28. Serafimova, I. M.; Hoggard, P. E. The photochemistry of chloro(triphenylphosphine)gold(I) and trichlorotriphenylphosphine)gold(III) in chloroform. *Inorg. Chim. Acta* **2002**, *338*, 105-110.

29. Bayler, A.; Schier, A.; Schmidbaur, H. Four-coordinate gold(I), silver(I), and copper(I) complexes with a large-span chiral ditertiary phosphine ligand. *Inorg. Chem*. **1998**, *37*, 4353-4359.

30. Thompson, J. F.; Scolyer, R. A.; Kefford, R. F. Cutaneous melanoma. *Lancet* **2005**, *365*, 687-701.

31. Grossman, D.; Altieri, D. C. Drug resistance in melanoma: mechanisms, apoptosis and new potential therapeutic targets. *Cancer Metastasis Rev.* **2001**, *20*, 3-11.

32. Berners-Price, S. J.; Bowen, R. J.; Galettis, P.; Healy, P. C.; McKeage, M. J. Structural and solution chemistry of gold(I) and silver(I) complexes with bidentate pyridil phosphines: Selective antitumor agents. *Coord. Chem. Rev.* **1999**, *185-186*, 823-826.

33. Mirabelli, C. K.; Hill, D. T.; Faucette, L. F.; McCabe, F. L.; Girard, G. R.; Bryan, D. B.; Sutton, B. M.; Barus, J. O; Crooke, S. T.; Johnson, R. K. Antitumor activity of bis(diphenylphosphino)alkanes, their gold(I) coordination complexes, and related compounds. *J. Med. Chem.* **1987**, *30*, 2181-2190.

34. Berners-Price, S. J.; Mirabelli, C. K.; Johnson R. K.; Mattern, M.R.; McCabe, F. L.; Faucette, L. F.; Sung, C. –M.; Mong, S. –M.; Sadler, P. J.; Crooke, S. T. In vivo antitumor activity and in vitro cytotoxic properties of bis[1,2-bis(diphenylphosphino)-ethane]gold(I) chloride. *Cancer Res.* **1986**, *46*, 5486-5493.

35. Struck, R. F.; Shealy, Y. F. Tertiary phosphines and phosphine oxides containing a 2-haloethyl group. *J. Med. Chem.* **1966**, *9*, 414-416.

36. Ronconi, L.; Marzano, C.; Zanello, P.; Corsini, M.; Miolo, G.; Macca, C.; Trevisan, A.; Fregona, D. Gold (III) Dithiocarbamate derivatives for the treatment of cancer : solution chemistry, DNA binding, and hemolytic properties. *J. Med. Chem.* **2006**, *49*, 1648-1657.

37. De Wall, S. L.; Painter, C.; Stone, J. D.; Bandaranayake, R.; Wiley, D. C.; Mitchison, T. J.; Stern, L. J.; DeDecker, B. S. Noble metals strip peptides from class II MHC proteins. *Nature Chem. Biol.* **2006**, *2*, 197-201.

38. Goebel, C.; Kubicka-Muranyi, M.; Tonn, T.; Gonzalez, J.; Gleichmann, E. Phagocytes render chemicals immunogenic: oxidation of gold(I) to the T cell-sensitizing gold(III) metabolite generated by mononuclear phagocytes. *Arch. Toxicol.* **1995,** *69*, 450–459.

39. Shaw III, C. F.; Schraa, S.; Gleichmann, E.; Grover, Y. P.; Dunemann, L.; Jagarlamudi, A. Redox chemistry and $[Au(CN)_2]^-$ in the formation of gold metabolites. *Metal Based Drugs* **1994**, *1*, 351–362.

40. Senko, M. W. IsoPro Isotopic Abundance Simulator, v. 2.1; National High Magnetic Field Laboratory, Los Alamos National Laboratory, Los Alamos, NM.

41. Camalli, M.; Spagna, R. CAOS program. *J. Applied Crystallogr.* **1994**, *27,* 861-862.

42. Delley, B. An all-electron numerical method for solving the local density functional for polyatomic molecules. *J. Chem. Phys.* **1990**, *92*, 508-517.

43. Caruso, F.; Rossi, M.; Opazo, C.; Pettinari, C. Structural features of antitumor gold(I)-phosphine derivatives analyzed with theoretical methods. *J. Arg. Chem. Soc.* **2004**, *92*, 119-124.

44. Perdew, J. P.; Chevary, J. A.; Vosko, S. H.; Jackson, Koblar A.; Pederson, Mark R.; Singh, D. J.; Fiolhais, C. Atoms, molecules, solids, and surfaces: applications of the generalized gradient approximation for exchange and correlation. *Phys. Rev. B: Cond. Mat. Mater. Phys.* **1992**, *46*, 6671-6687.

45. Delley, B. Fast calculation of electrostatics in crystals and large molecules. *J. Phys. Chem.* **1996**, *100*, 6107-6110.

46. Badaracco, G.; Corsi, A.; Maisto, A.; Natali, P. G.; Storace, G.; Zupi, G. Expression of tumor-associated antigens and kinetic profile of two melanoma cell lines. *Cytometry* **1981**, *2*, 63-69.

47. Supino, R.; Mapelli, E.; Sanfilippo, O.; Silvestro, L. Biological and enzymatic features of human melanoma clones with different invasive potential. *Melanoma Res.* **1992**, *2*, 377-384.

48. Formelli, F.; Rossi, C.; Supino, R; Parmiani, G. In vivo characterization of a doxorubicin resistant B16 melanoma cell line. *Br. J. Cancer*, **1986**, *54*, 223-33.

49. Perez, R. P.; Godwin, A. K.; Handel, L. M.; Hamilton, T. C. A comparison of clonogenic, microtetrazolium and sulforodamine B assays for determination of cisplatin cytotoxicity in human ovarian carcinoma cell lines. *Eur. J. Cancer* **1993**, *29A*, 395-399.

ACKNOWLEDGMENTS. Università di Camerino, Fondazione Carima, Vassar College Research Committee. Cristian Opazo at Vassar College SCIVIS lab for support with DMol3 program.

Supporting Information Available. DFT molecular coordinates for chelate (Table S1) and non-chelate (Table S2) converged structures of $[Au_2(DPPP)_2Cl]^+$, and for $[\{AuCl(PPh_3)\}_2(\mu_2\text{-DIPHOS})]$ (Table S3). X-ray data, fractional coordinates and displacement parameters of $[\{AuCl(PPh_3)\}_2(\mu_2\text{-DIPHOS})]$ (Tables S4-S6). Full lists of X-ray bond distances and angles for $[\{AuCl(PPh_3)\}_2(\mu_2\text{-DIPHOS})]$ (Tables S7-S8). List of Au-DIPHOS chelate refcodes, for 3-coordinate metal found in the CSD (Table S9). DFT drawing of $[\{AuCl(PPh_3)\}_2(\mu_2\text{-DIPHOS})]$, (Figure S1). This material is available free of charge via the Internet at http://pubs.acs.org.

Table 1. Selected structural parameters of [{AuCl(PPh_3)}$_2$(μ_2-DIPHOS)].

Method	X-ray	DFT
Au - P(Ph)	2.313(4)	2.483
Au -P(DIPHOS)	2.323(4)	2.485
Au -Cl	2.632(5)	2.538
P(DIPHOS) - Au - P(Ph)	145.2(2)	131.0
Cl- Au - P(Ph)	108.9(2)	115.9
Cl - Au - P(DIPHOS)	105.8(2)	113.0

Table 2. Cytotoxic activity of gold complexes in human melanoma cell lines

	IC_{50} (μM)	
	[{AuCl(PPh_3)}$_2$(μ_2-DIPHOS)]	[Au(DPPP)(PPh_3)Cl]
JR8	28 ± 0.33	0.8 ± 0.11
SK-MEL-5	2.7 ± 0.11	1.0 ± 0.56
2/60	5.5 ± 0.085	1.7 ± 0.47

IC_{50} values were determined graphically from the growth inhibition curves obtained after a 48-h exposure of the cells to each drug. Data represent mean values ± SD of three independent experiments. Values for [Au(DPPP)(PPh_3)Cl] are taken from the literature.[20]

Figure Captions

Figure 1. X-ray crystal structure of [{AuCl(PPh_3)}$_2$(μ_2-DIPHOS)] showing ellipsoid displacement parameters. For 2 Ph groups only the *ipso* carbons are shown and all H-atoms are omitted for clarity; P black, C grey, Au white, Cl light grey. The inversion center of this molecule is located in the ethylene bridge between C31 and C31'.

Figure 2. Graph from 13 non-chelate gold(I)-DIPHOS crystal structures found at the CSD (listed in Supporting information available); some of these species have more than one independent molecular unit.

Figure 3. Dose-response curves of human melanoma cell lines (♦ JR8, ■ 2/60, ▲ SK-MEL-5) exposed to [{AuCl(PPh_3)}$_2$(μ_2-DIPHOS)] for 48 h. Points represent mean values ± SD of three independent experiments.

Figure 4. Dose-response curves obtained from B16V cells exposed to [{AuCl(PPh_3)}$_2$(μ_2-DIPHOS)] (■) and [Au(DPPP)(PPh_3)Cl] (●) for 48 h. Points represent the mean ± SD of four independent experiments.

Figure 5. A non-chelate structure of $[Au_2(DPPP)_2Cl]^+$ obtained with DFT methods and having aromatic H atoms omitted for clarity; P orange, C grey, H white, Au purple, Cl green.

Figure 6. The chelate structure of $[Au_2(DPPP)_2Cl]^+$ obtained with DFT methods and having H atoms omitted for clarity ; P orange, C grey, H white, Au purple, Cl green.

Figure 7. Geometry optimized triangular $[Au^I(DMPP)(PMet_3)]^+$ complex; P orange, C grey, H white, Au purple.

Figures

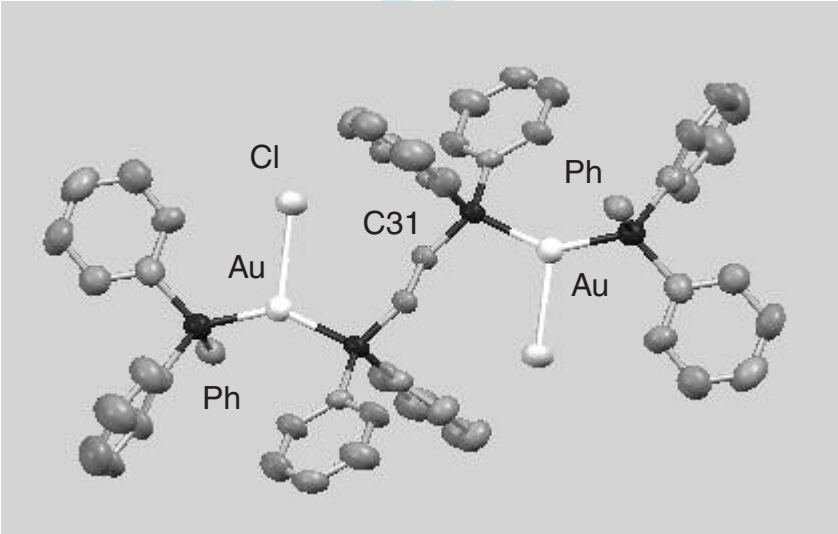

Figure 1.

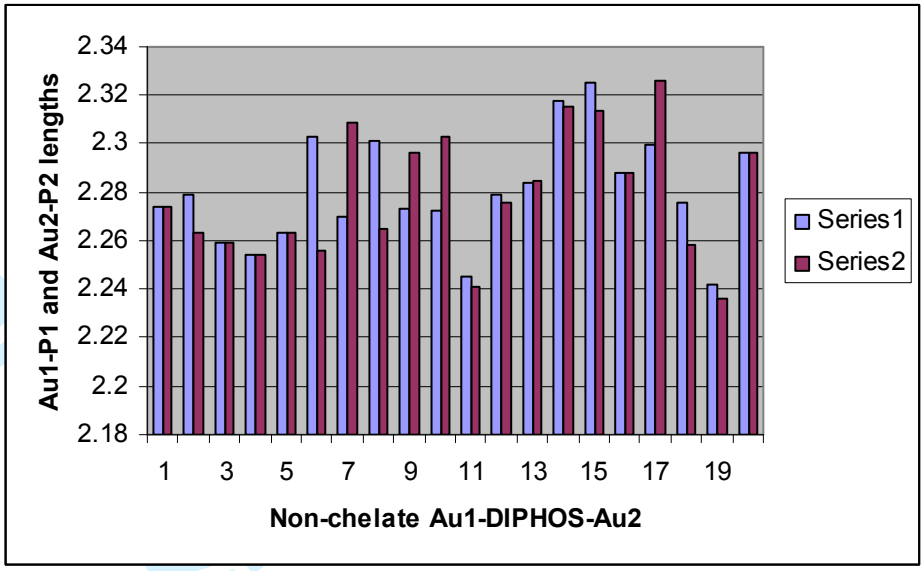

Figure 2.

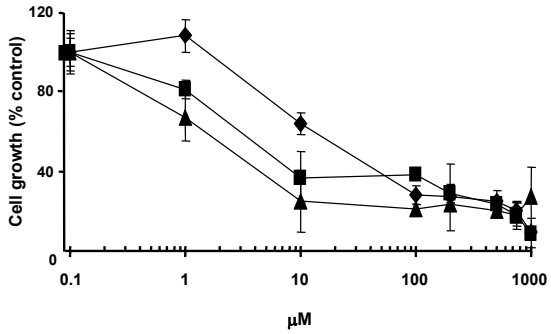

Figure 3.

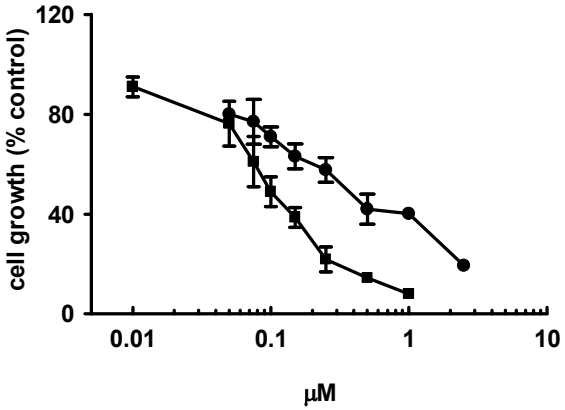

Figure 4.

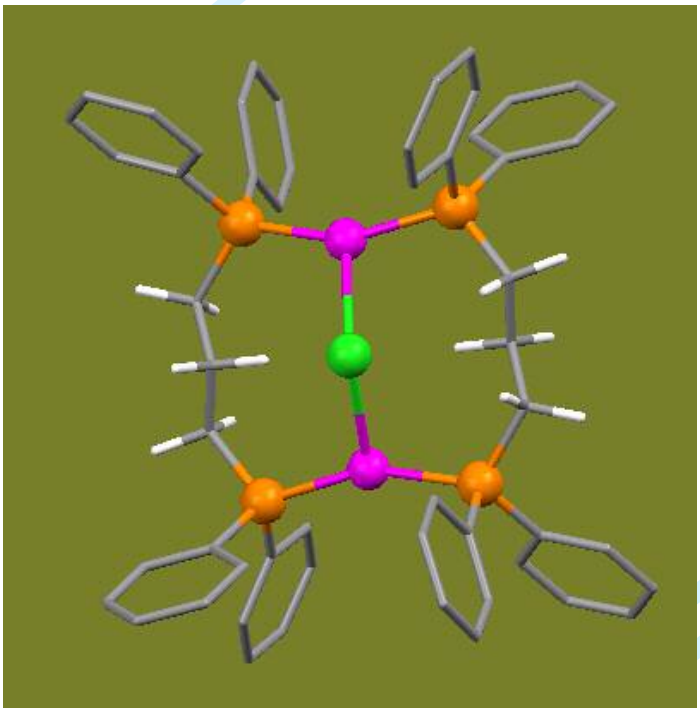

Figure 5.

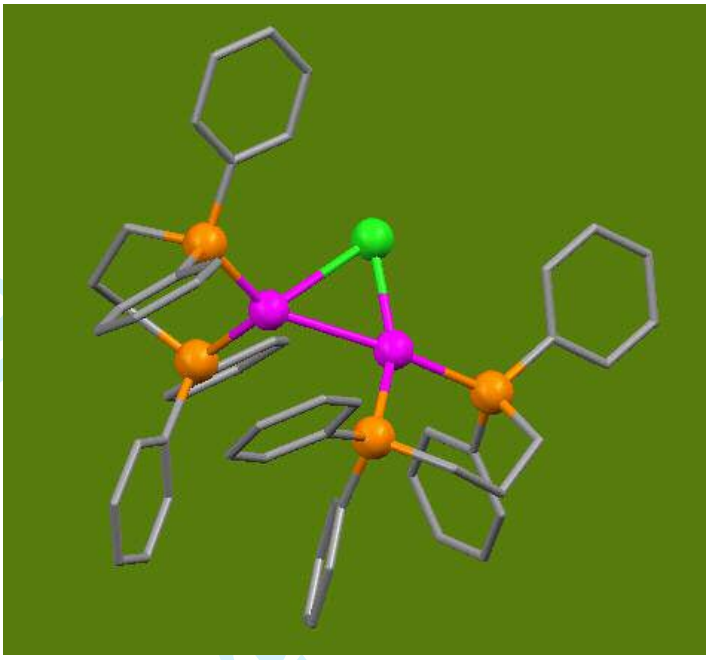

Figure 6.

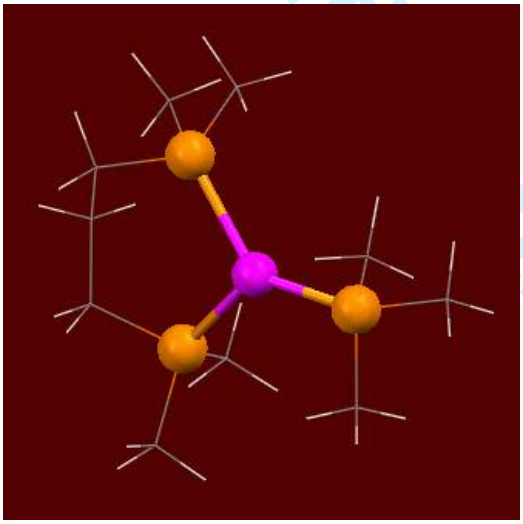

Figure 7

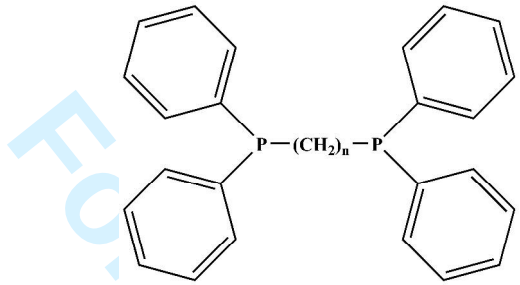

DIPHOS: n = 2; DPPP: n = 3

Scheme 1: Diphosphine ligands used in this work.

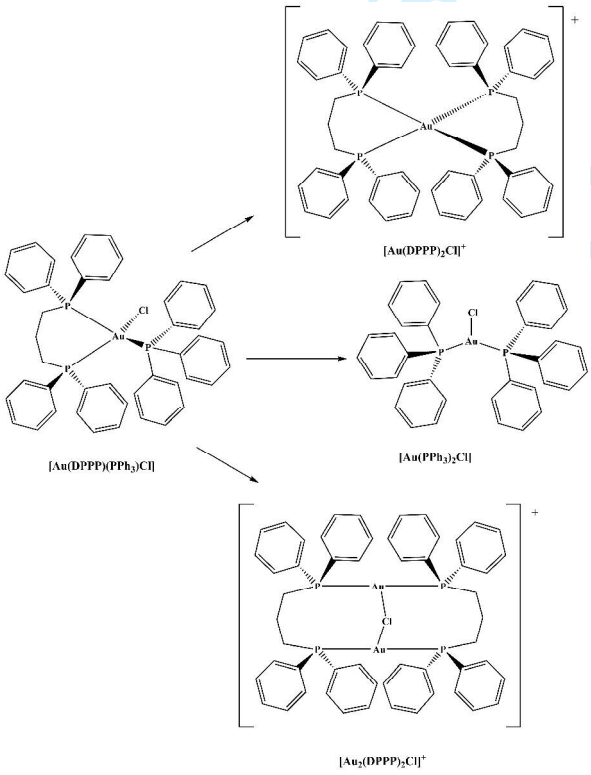

Scheme 2: Decomposition of [Au(DPPP)(PPh_3)Cl].

$$[Au(DPPP)(PPh_3)Cl] \leftrightarrows [Au(DPPP)_2]Cl + [Au(PPh_3)_2Cl]$$

Scheme 3:

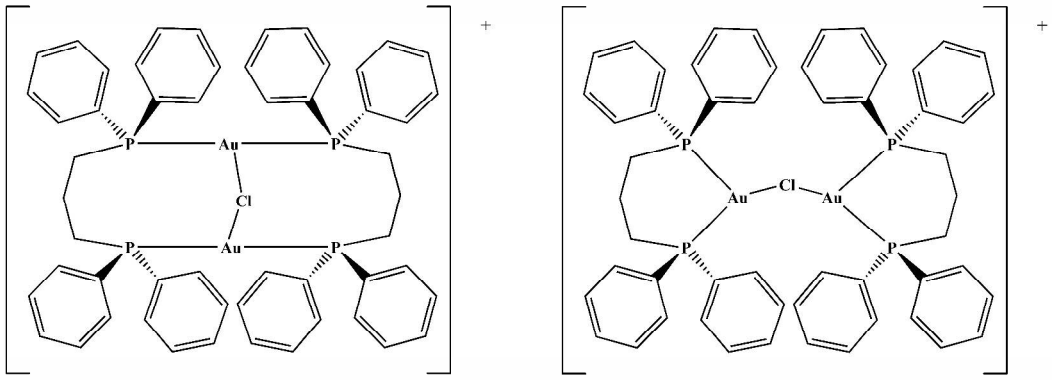

Scheme 4: Non-chelate and chelate connectivity of $[Au_2(DPPP)_2Cl]^+$.

$$[Au^{I}(DMPP)(PMet_3)]^+ + 2[H]^+ + 4[OCl]^- \rightarrow [Au^{III}Cl_4]^- + DMPPO_2 + PMet_3O + H_2O$$

Scheme 5: A modeled hypochlorite oxidation for Au(I) to Au(III).

TOC

The naturally occurring endogenous hypochlorite anion may oxidize the melanoma antitumor compound $[Au^{I}(DPPP)(PPh_3)Cl]$ forming $[Au^{III}Cl_4]^-$ and phosphine oxides; DFT calculated DeltaG is -126.7 kcal/mol for a related model reaction.

This non-chelate Au(I)-diphosphine species $[\{AuCl(PPh_3)\}_2(\mu_2\text{-DIPHOS})]$

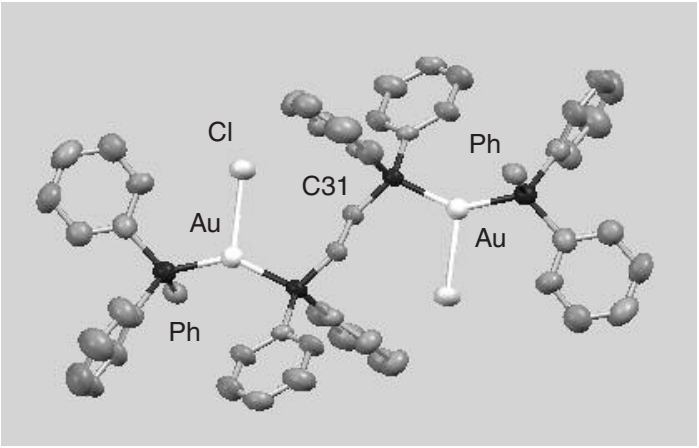

is slightly less active than the chelate $[Au(DPPP)(PPh_3)Cl]$ against several *in vitro* melanoma cell lines.